*Supporting Information for:*

# Bimodel effects on lipid droplets induced in cancer and non-cancer cells by chemotherapy drugs as revealed by green-emitting BODIPY fluorescent probe

Artūras Polita,*[a] Rokas Žvirblis,[b] Jelena Dodonova-Vaitkūnienė,[c] Arun Prabha Shivabalan,[a] Karolina Maleckaitė [d] and Gintaras Valinčius [a]

[a.] *Life Sciences Center, Institute of Biochemistry, Vilnius University, Saulėtekio av. 7, Vilnius, LT-10257, Lithuania. E-mail: arturas.polita@gmc.vu.lt.*
[b.] *Life Sciences Center, Institute of Biotechnology, Vilnius University, Saulėtekio av. 7, Vilnius, LT-10257, Lithuania.*
[c.] *Institute of Chemistry, Faculty of Chemistry and Geosciences, Vilnius University, Naugarduko st. 24, Vilnius, LT-03225, Lithuania.*
[d.] *Center of Physical Sciences and Technology, Saulėtekio av. 3, Vilnius, LT-10257, Lithuania.*

## Table of Contents

## Absorption, steady-state and time-resolved fluorescence spectra of BODIPY-LD in various solvents (methanol, DMSO, dichloromethane, chloroform, toluene, cyclohexane)

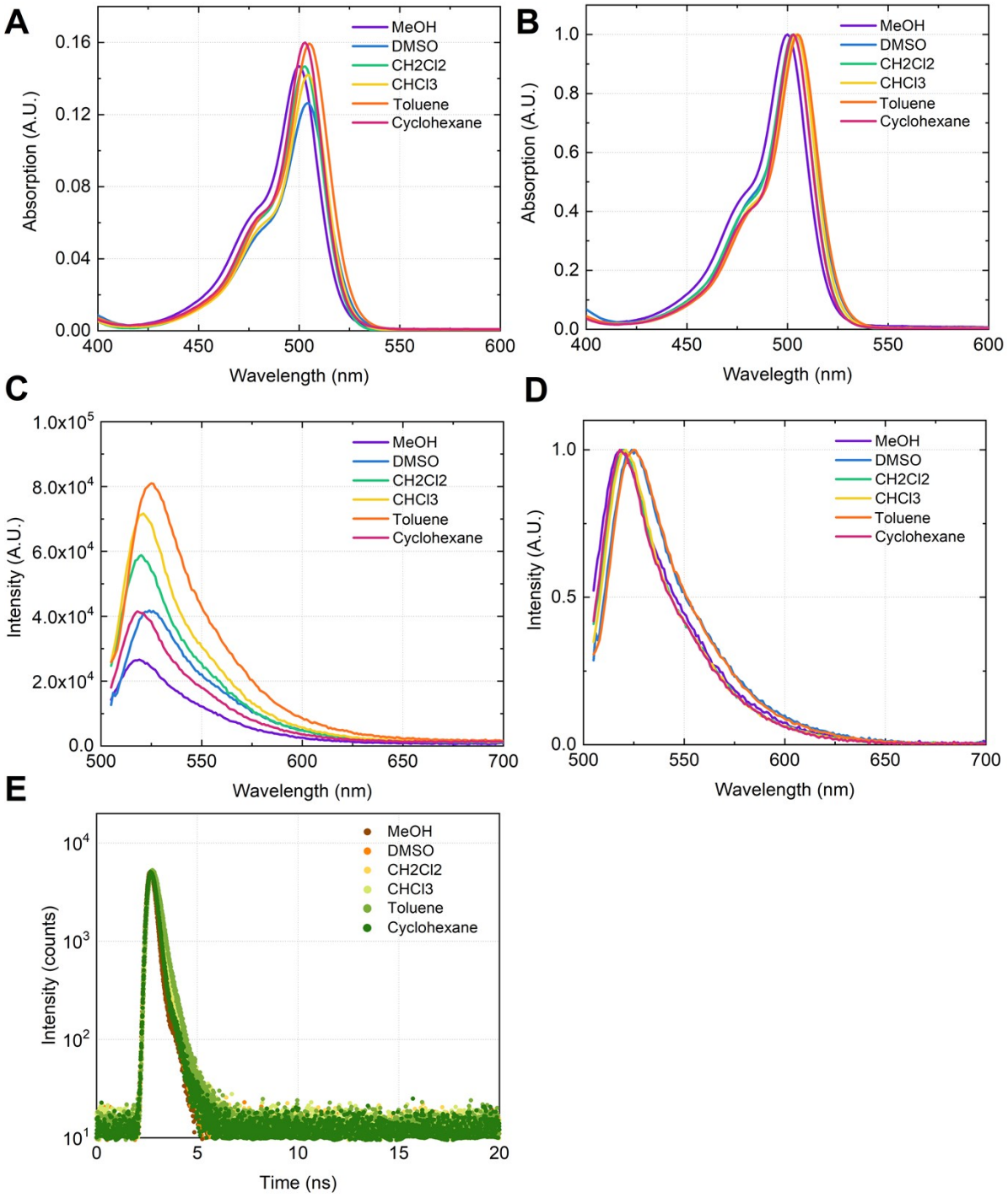


**Figure S1**. (A) Relative absorption spectra of BODIPY-LD in cyclohexane, toluene, chloroform, dichloromethane, DMSO and methanol. (B) Normalized absorption spectra of BODIPY-LD in cyclohexane, toluene, chloroform, dichloromethane, DMSO and methanol. (C) Relative steady-state fluorescence spectra of BODIPY-LD in cyclohexane, toluene, chloroform, dichloromethane, DMSO and methanol. (D) Normalized steady-state fluorescence spectra of BODIPY-LD in cyclohexane, toluene, chloroform, dichloromethane, DMSO and methanol. (E) Time-resolved fluorescence decays of BODIPY-LD in cyclohexane, toluene, chloroform, dichloromethane, DMSO and methanol.

BODIPY-LD was dissolved at a concentration of 2 μM in a variety of solvents of varying polarity (Fig. S1). We did not observe any visible aggregation of the dye in the tested solvents. Additionally, the absence of red bands in the steady-state emission spectra indicates that BODIPY-LD does not form aggregates in low or high polarity solvents (Fig. S1C and S1D). The time-resolved fluorescence decays of BODIPY-LD in cyclohexane, toluene, chloroform, dichloromethane, DMSO and methanol were monoexponential (Fig. S1E). The precise fluorescence lifetimes are presented in Table S1.

| **Solvent** | **Fluorescence lifetime τ, ps** | **χ2** |
|---|---|---|
| Methanol | 92.71 | 1.25 |
| DMSO | 153.27 | 1.274 |
| Dichloromethane | 176.62 | 1.246 |
| Chloroform | 226.72 | 1.191 |
| Toluene | 247.25 | 1.226 |
| Cyclohexane | 147.21 | 1.256 |

**Table S1**. Precise monoexponential fluorescence lifetimes of BODIPY-LD in cyclohexane, toluene, chloroform, dichloromethane, DMSO and methanol at room temperature.

## BODIPY-PM absorption, steady-state and time-resolved fluorescence spectra in methanol-glycerol mixtures

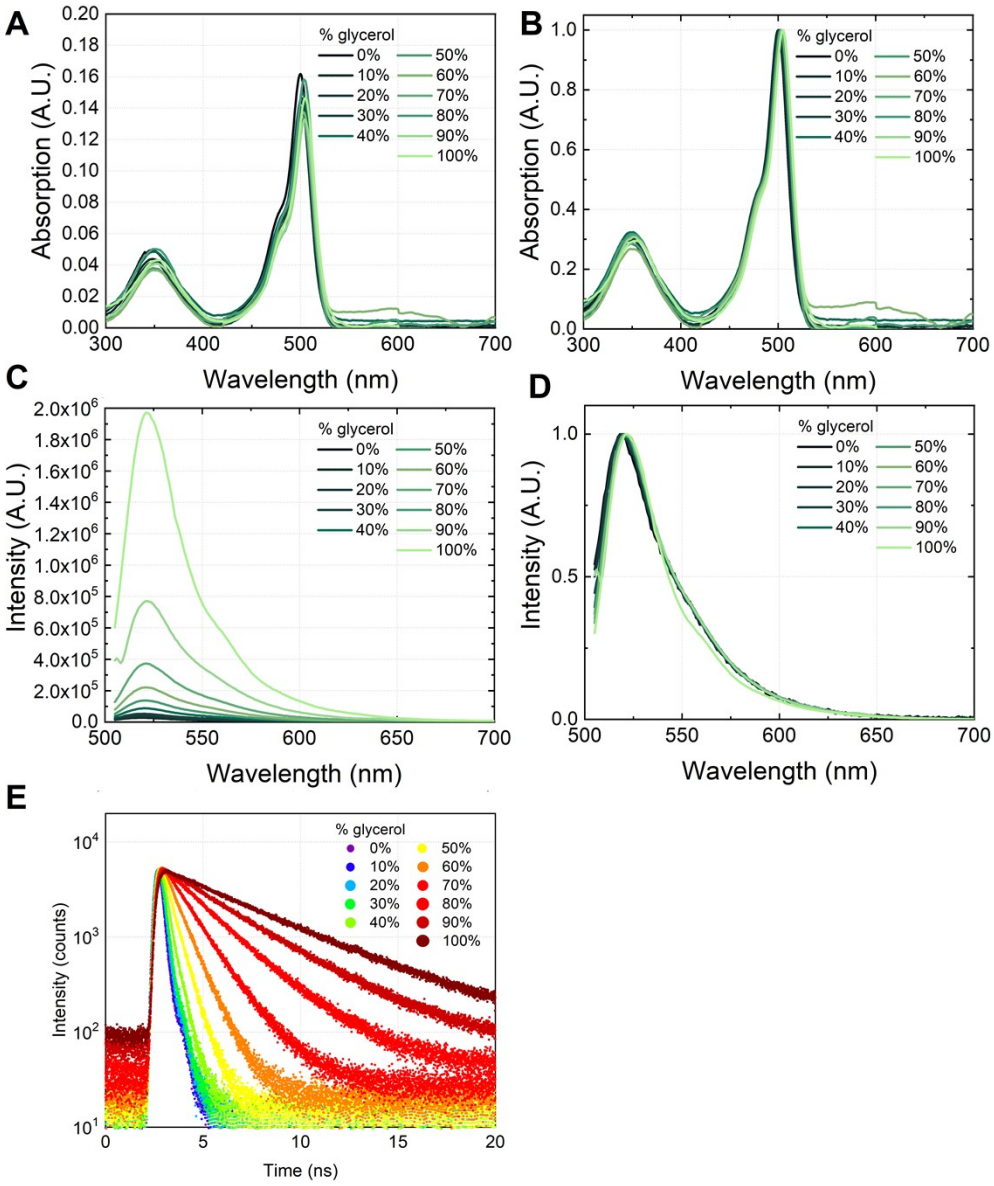


**Figure S2**. (A) Relative absorption spectra of BODIPY-LD in methanol-glycerol mixtures, starting from pure methanol. (B) Normalized absorption spectra of BODIPY-LD in methanol-glycerol mixtures, starting from pure methanol. (C) Relative steady-state fluorescence spectra of BODIPY-LD in methanol-glycerol mixtures, starting from pure methanol. (D) Normalized steady-state fluorescence spectra of BODIPY-LD in methanol-glycerol mixtures, starting from pure methanol. (E) Time-resolved fluorescence decays of BODIPY-LD in methanol-glycerol mixtures, starting from pure methanol.

BODIPY-LD was dissolved at a concentration of 2 µM in methanol-glycerol mixtures, starting from pure methanol (MeOH) and ending with pure glycerol (Gly) (Fig. S2). The absorption spectra of BODIPY-LD feature slight red-shift with increase in glycerol concentration, from peak maximum at 500 nm in methanol to peak maximum of 505 nm in pure glycerol (Fig. S2B). We did not observe any visible aggregation of the dye in the tested mixtures. The time-resolved fluorescence decays of BODIPY-LD in methanol and methanol-glycerol mixtures up to 60% glycerol were monoexponential, starting from 40% methanol-60% glycerol mixtures, the fluorescence decays become biexponential (Fig. S2E). The precise fluorescence lifetimes and viscosities of the mixtures are presented in Table S2.

| Composition | $\tau_1$, ps | $\tau_2$, ps | $A_1$, % | $A_2$, % | Intensity-weighted fluorescence lifetime, ps | Viscosity, cP | χ2 |
|---|---|---|---|---|---|---|---|
| Methanol | 92.71 | | 100 | | | 0.627 | 1.25 |
| MeOH-10% Gly | 109.24 | | 100 | | | 1.0 | 1.364 |
| MeOH-20% Gly | 136.92 | | 100 | | | 1.8 | 1.309 |
| MeOH-30% Gly | 176.27 | | 100 | | | 3.33 | 1.254 |
| MeOH-40% Gly | 274.31 | | 100 | | | 6.46 | 1.215 |
| MeOH-50% Gly | 471.6 | | 100 | | | 14.02 | 1.355 |
| MeOH-60% Gly | 537.97 | 968.24 | 60.3 | 39.7 | 771.27 | 30.73 | 1.157 |
| MeOH-70% Gly | 735.74 | 1470 | 39.84 | 60.16 | 1284.20 | 72.96 | 1.062 |
| MeOH-80% Gly | 1022.94 | 2416.89 | 29.0 | 71.0 | 2211.38 | 183.43 | 1.118 |
| MeOH-90% Gly | 863.55 | 3427.08 | 15.86 | 84.14 | 3310.82 | 513.36 | 1.126 |
| Glycerol | 779.14 | 4717.7 | 10.97 | 89.03 | 4639.13 | 1457.55 | 1.128 |

**Table S2**. Precise fluorescence lifetimes of BODIPY-LD in methanol-glycerol mixtures at room temperature.

## Steady-state and time-resolved fluorescence spectra of BODIPY-LD in DOPC and DOPC/DPPC/Chol (1/5/5) LUVs

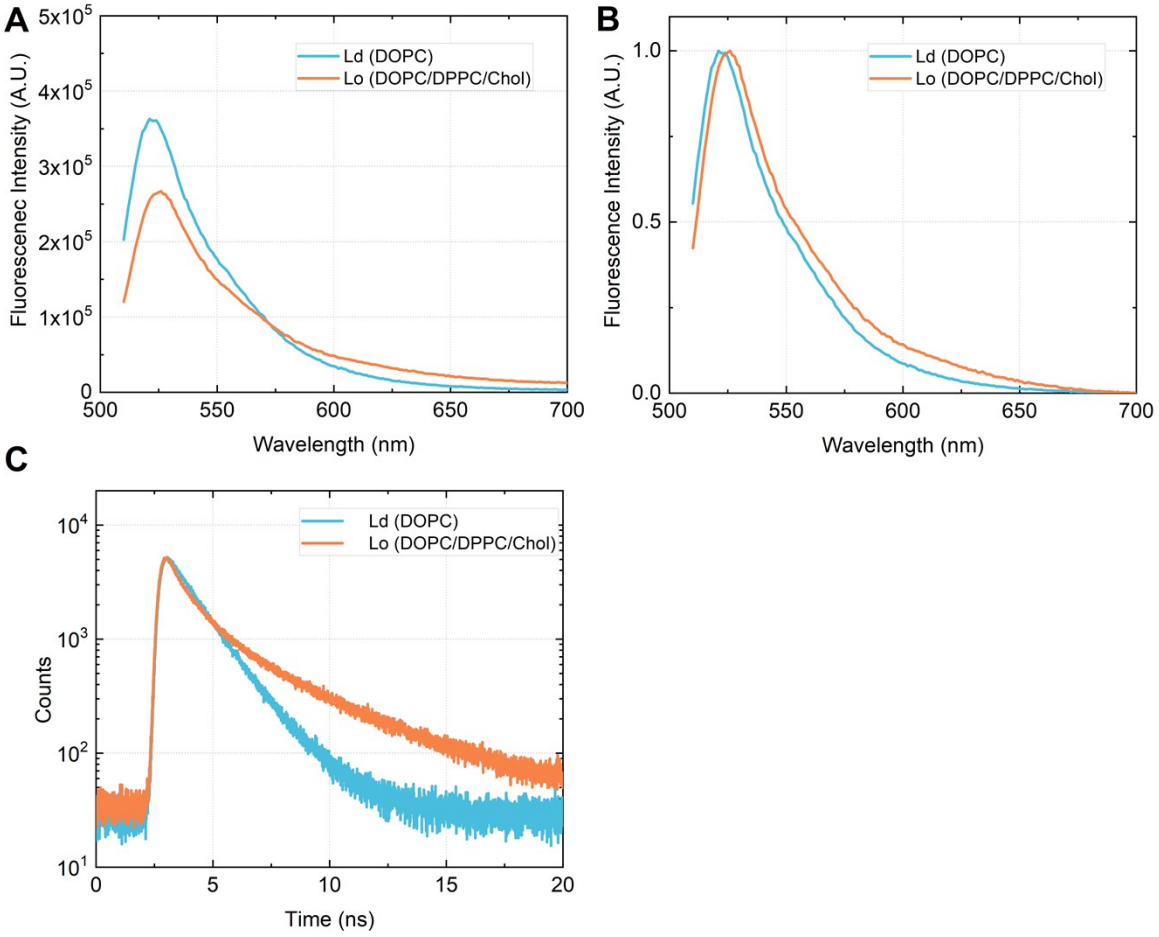


**Figure S3**. (A) Relative steady-state fluorescence spectra of BODIPY-LD in Ld (DOPC) and Lo (DOPC/DPPC/Chol 1/5/5) LUVs. (B) Normalized steady-state fluorescence spectra of BODIPY-LD in Ld (DOPC) and Lo (DOPC/DPPC/Chol 1/5/5) LUVs. (C) Time-resolved fluorescence decays of BODIPY-LD Ld (DOPC) and Lo (DOPC/DPPC/Chol 1/5/5) LUVs.

LUVs with a diameter of 100nm were prepared in the Lo (DOPC/DPPC/Chol 1/5/5) and Ld (DOPC) phases. In LUVs, the BODIPY-LD to lipid ratio was 1:800. BODIPY-LD displays a slight red-shifted fluorescence spectra in Lo phase compared to Ld phase, with the fluorescence intensity maximum changing from 521nm in Ld to 526 nm in Lo phase (Fig. S3). In addition, the fluorescence intensity in Ld phase is about 1.5-times higher compared to the Lo phase (Fig. S3).

## Brightfield microscopy of A549 and HEK 293T cells stained with BODIPY-LD

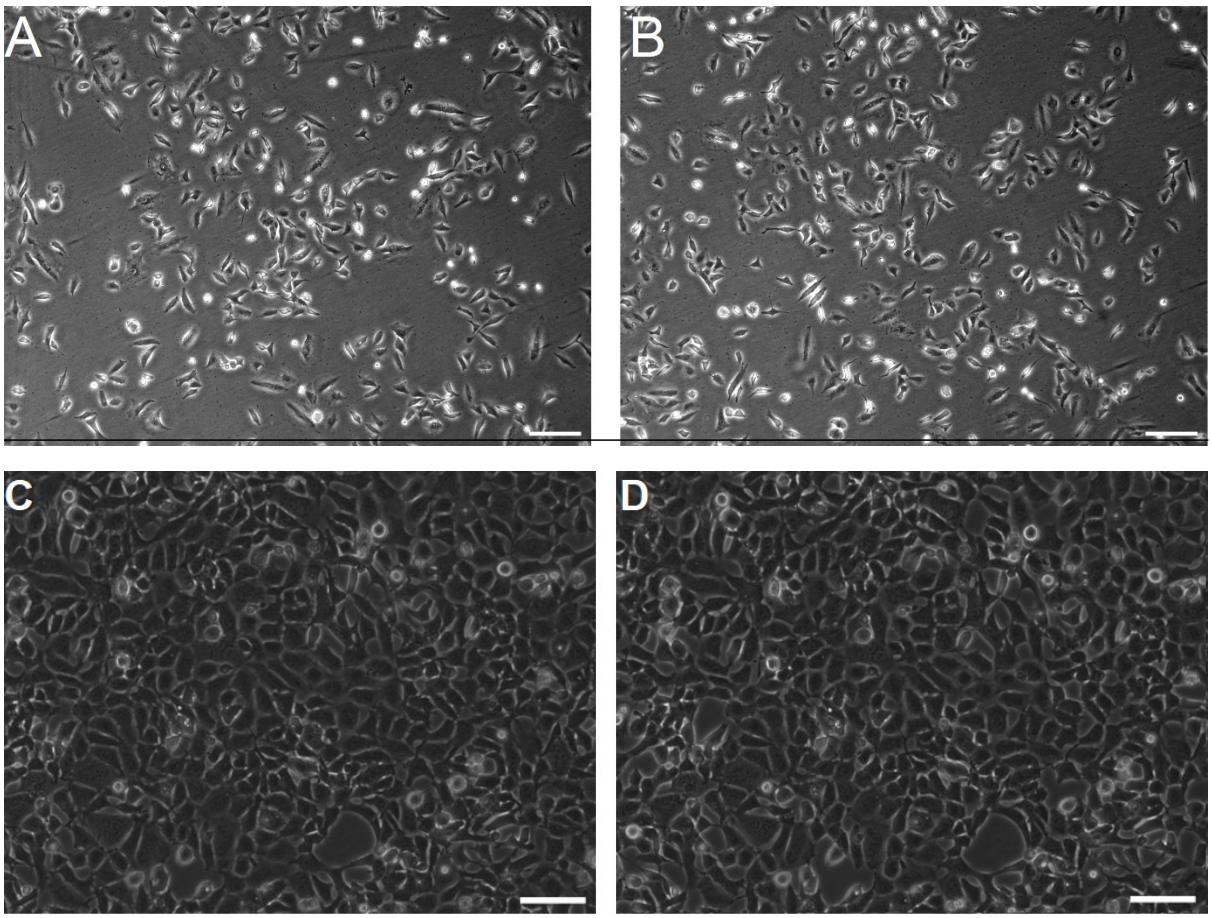


**Figure S4**. (A) Brightfield image of A549 human lung cancer cells before addition of BODIPY-LD, the cells display normal morphology, scale bar is 100 µm. (B) Brightfield image of A549 human lung cancer cells, stained with BODIPY-LD (5 µM), scale bar is 100 µm. (C) Brightfield image of HEK 293T human embryonic kidney cells before addition of BODIPY-LD, the cells display normal morphology, scale bar is 100 µm. (D) Brightfield image of HEK 293T human embryonic kidney cells, stained with BODIPY-LD (5 µM), scale bar is 100 µm.

We have performed brightfield imaging to determine if BODIPY-LD alters the morphology of human lung cancer A549 and human embryonic kidney HEK 293T cells. Both cell types displayed normal cell morphology after the addition of BODIPY-LD (5 µM) and incubation for 5-10 min. (Fig. S4).

## Confocal fluorescence intensity images of A549 cells stained with BODIPY-LD (DMSO, 1µM) showcasing the movement of LDs

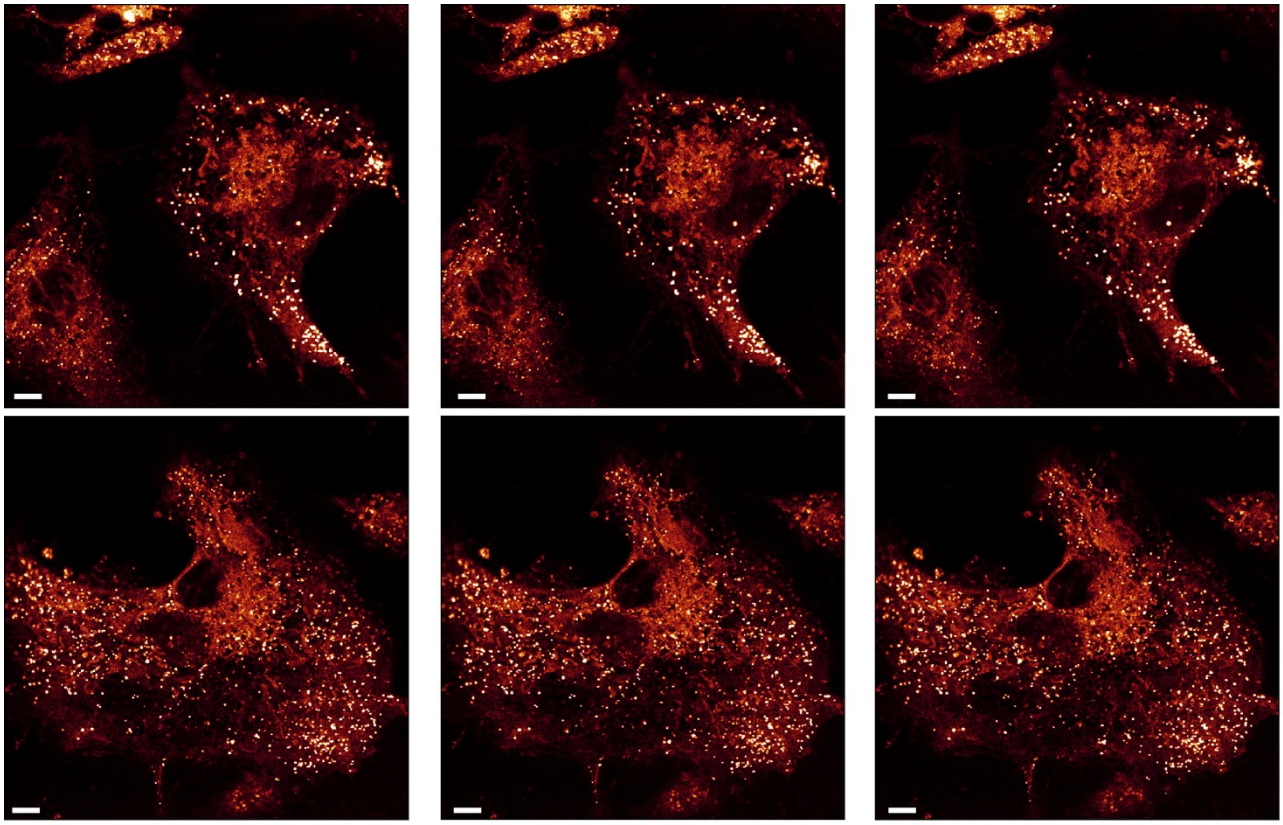

**Figure S5**. Confocal fluorescence intensity images of A549 cells stained with BODIPY-LD (DMSO, 1µM) showcasing the movement of LDs. Scale bar is 10 µm. The images were taken approximately 10 seconds apart.

We stained A549 cells for 5 min. with BODIPY-LD to showcase the movement of lipid droplets (Fig. S5). The lipid droplets can be seen moving slowly in the cytoplasm. Figure S5 in the gif format is presented below.

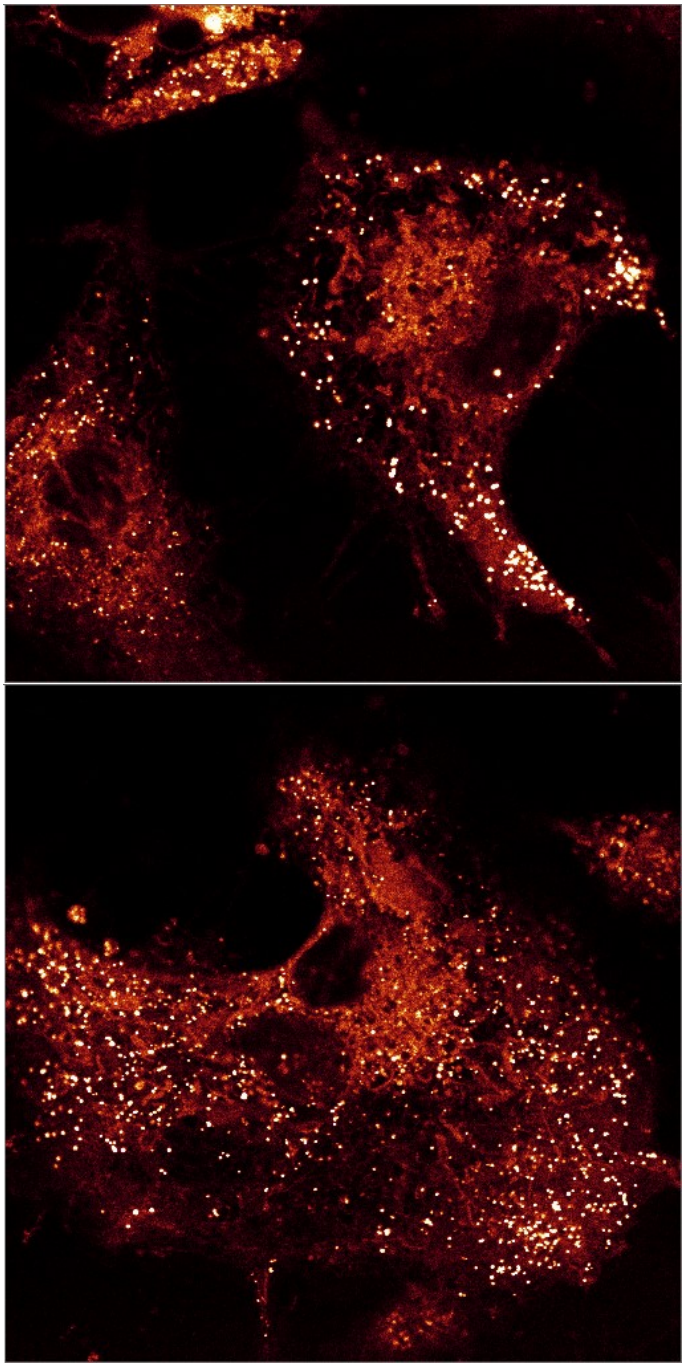

## Co-localisation of Nile Red and BODIPY-LD in A549 cells

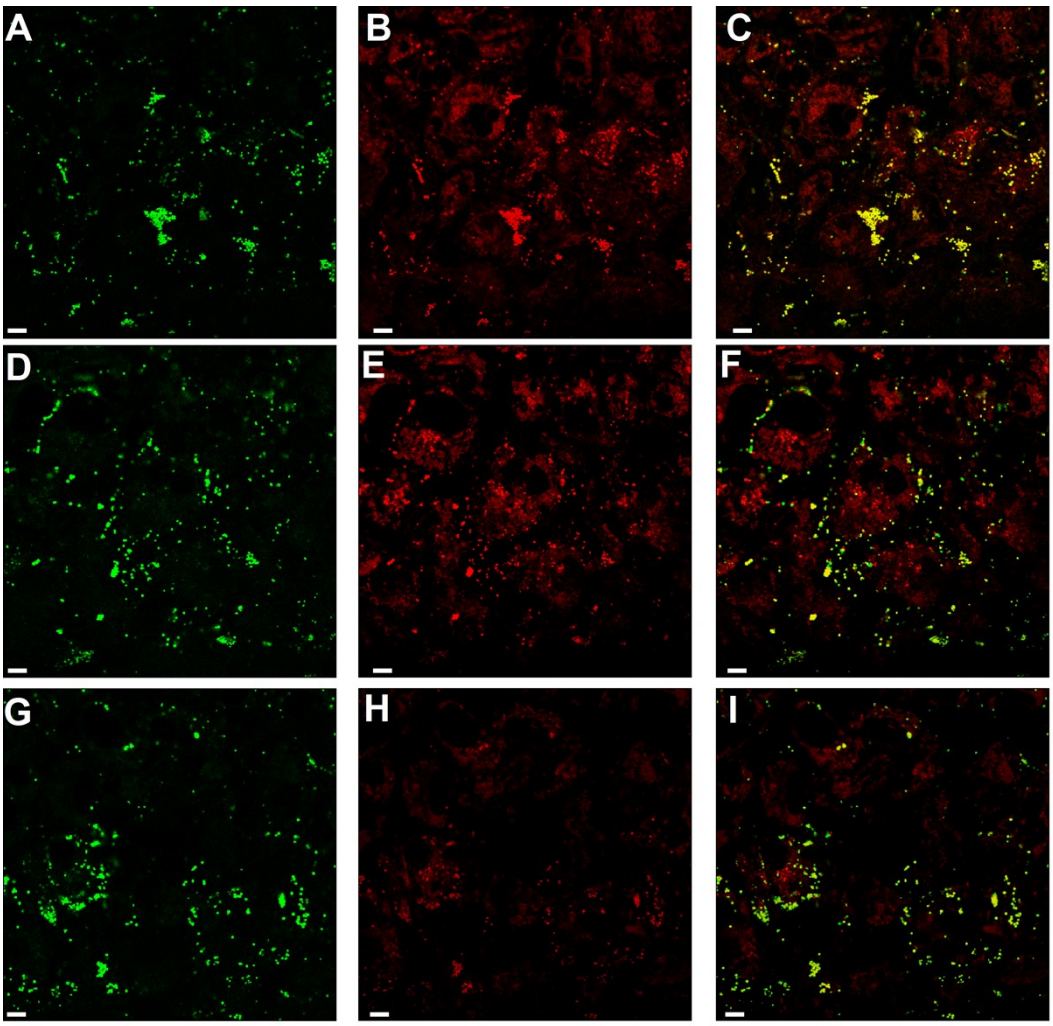


**Figure S6**. Confocal fluorescence intensity images of A549 cells stained with BODIPY-LD and Nile Red. (A), (D) and (G) BODIPY-LD fluorescence images. (B), (E) and (H) corresponding Nile Red fluorescence intensity images. (C), (F), and (I) merged images of BODIPY-LD and Nile-Red channels. Scale bar is 10 µm.

We have labelled A549 cells with BODIPY-LD and Nile Red - a known marker for lipid droplets (Fig. S6). The 488 nm laser line was used for BODIPY-LD excitation, and fluorescence intensity images were captured in the 505-550 nm window. The 553 nm laser excitation line was chosen for Nile Red, with fluorescence intensity measured at 650-750 nm. The two dyes appear to be co-localised in the same organelles. In addition, BODIPY-LD is much more selective for lipid droplets compared to Nile Red.

## Steady-state fluorescence spectra of BODIPY-LD in LDs

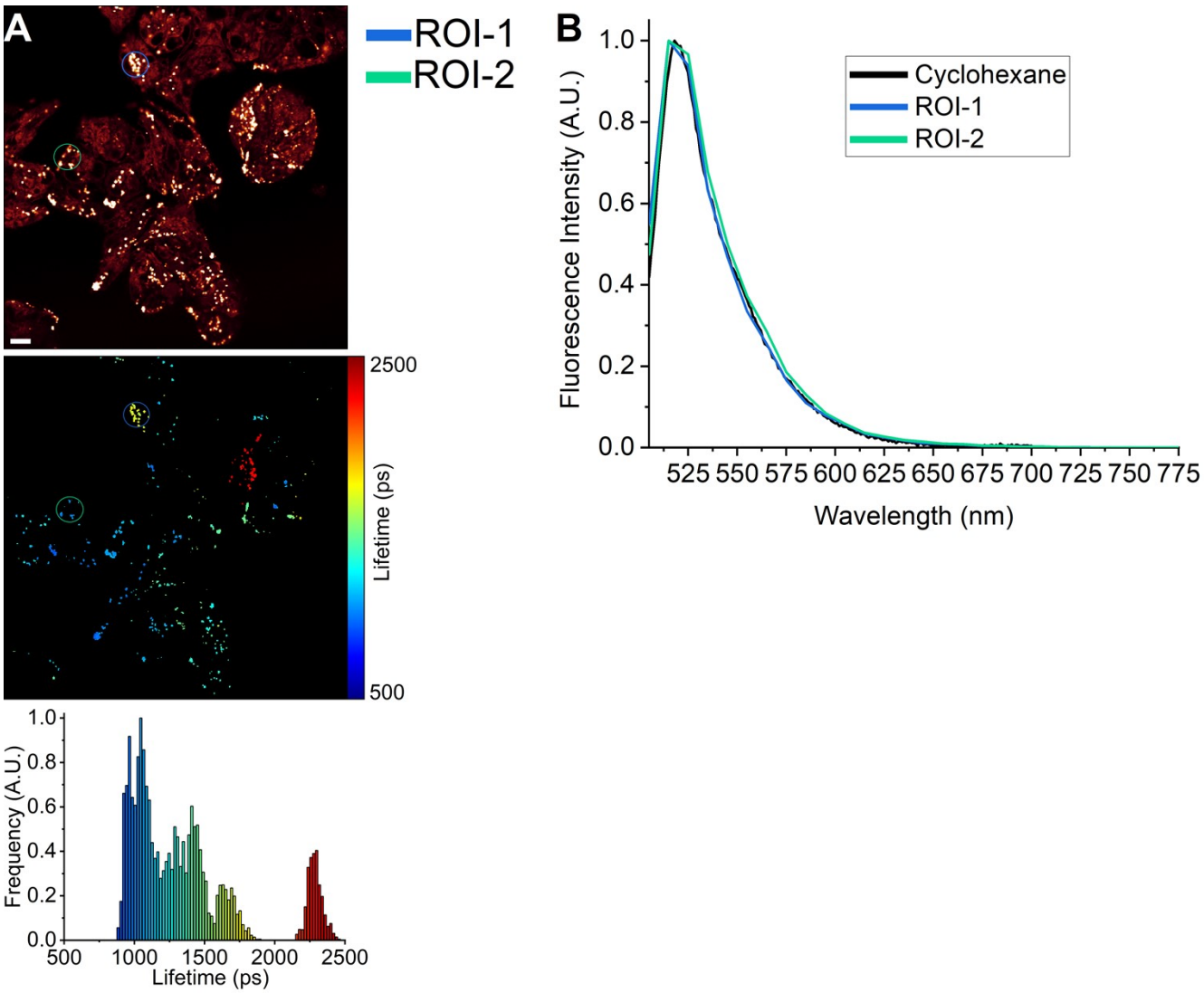


**Figure S7**. (A) FLIM of A549 cells stained with BODIPY-LD (1µM). Regions-of-interest (ROI) mark the areas from which the fluorescence spectra were selected. (B) Steady-state fluorescence spectra of BODIPY-LD in LDs and cyclohexane. Scale bar is 10 µm.

We have performed the lambda scan to record the steady-state fluorescence spectrum of BODIPY-LD in lipid droplets to confirm that no aggregation of the dye takes place (Fig. S7). The steady-state fluorescence spectra from two different regions of interest are shown in Fig. S7B together with the steady-state spectrum of cyclohexane for comparison. The corresponding regions of interest (ROIs) are shown in Fig. S7A together with the FLIM data.

## FLIM of BODIPY-LD stained LDs in A549 cells with etoposide $IC_{50}$ treatment

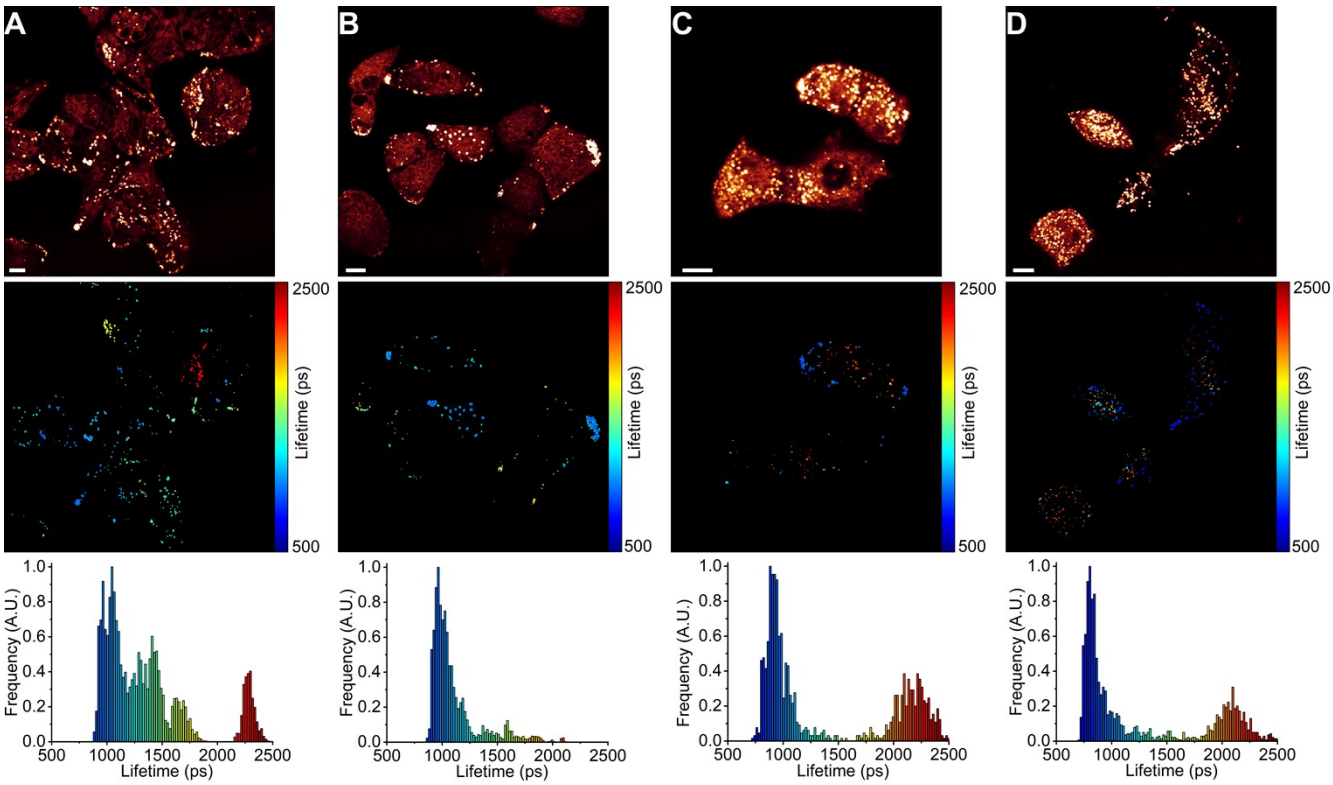


**Figure S8**. FLIM of BODIPY-LD in LDs of A549 cells (A), A549 cells treated with etoposide for 6 hrs. (B), A549 cells treated with etoposide for 24 hrs. (C), A549 cells treated with etoposide for 48 hrs. (D). The top panel shows images of fluorescence intensity. FLIM images are shown in the middle panel. The corresponding lifetime histograms are shown in the bottom panel. Scale bars are 10 µm.

A549 cells were treated with $IC_{50}$ concentrations of etoposide for 48 hours and imaged after 6, 24 and 48 hours (Fig. S8). The amount of viscous lipid droplets, with intensity-weighted fluorescence lifetimes of BODIPY-LD of more than 1500 ps, is reduced after 6 hrs. of etoposide treatment. However, highly viscous lipid droplets reappear after 24 hrs. of etoposide treatment. Furthermore, highly non-viscous lipid droplets, with BODIPY-LD intensity-weighted fluorescence lifetimes of 750 ps, begin to form. In addition, the number of lipid droplets in single cells sharply increases after 24 hrs. of etoposide treatment. Finally, after 48 hrs. of etoposide treatment, all A549 cells possess highly viscous and highly non-viscous lipid droplets.

## FLIM of BODIPY-LD stained LDs in HEK 293T cells with etoposide $IC_{50}$ treatment

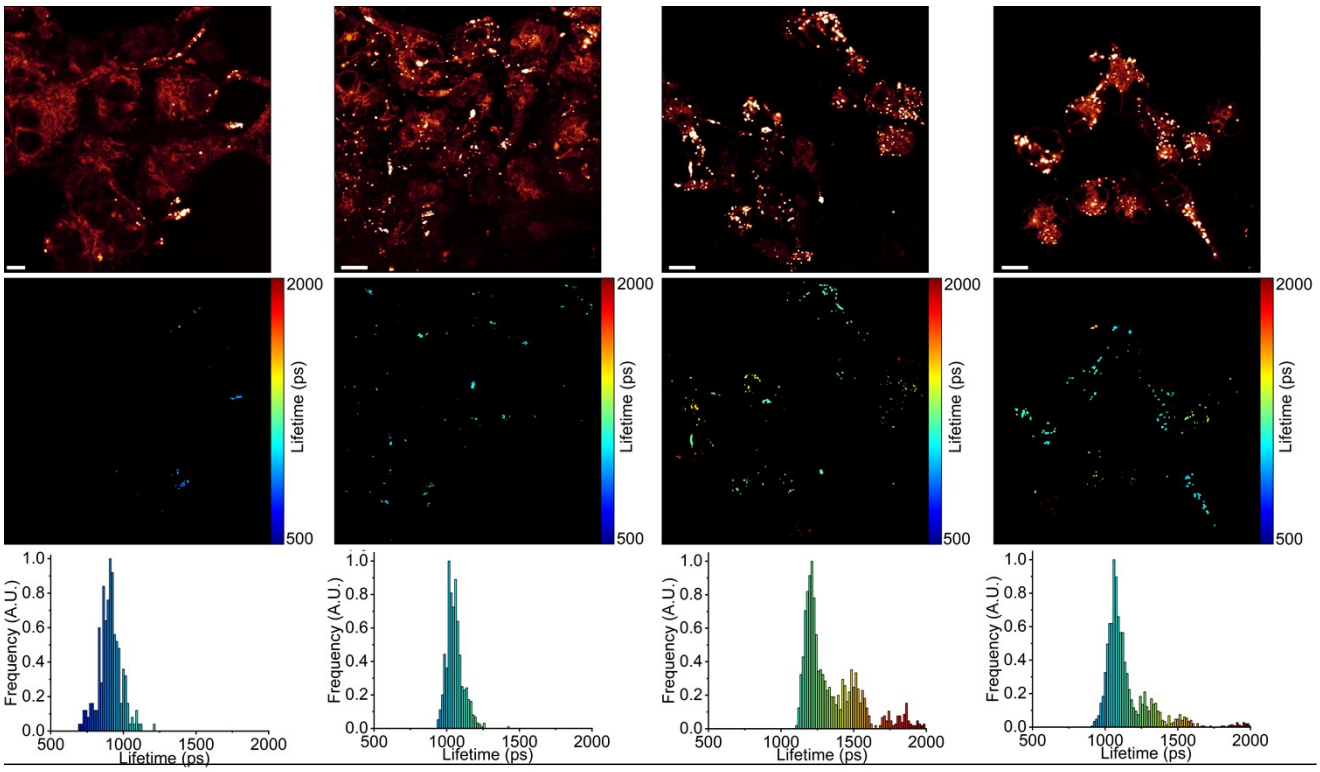


**Figure S9**. FLIM of BODIPY-LD in LDs of HEK 293T cells (A), HEK 293T cells treated with etoposide for 6 hrs. (B), HEK 293T cells treated with etoposide for 24 hrs. (C), HEK 293T cells treated with etoposide for 48 hrs. (D). The top panel shows images of fluorescence intensity. FLIM images are shown in the middle panel. The corresponding lifetime histograms are shown in the bottom panel. Scale bars are 10 µm.

HEK 293T cells were treated with $IC_{50}$ concentrations of etoposide for 48 hours and imaged after 6, 24 and 48 hours (Fig. S9). The number of lipid droplets in HEK 293T cells significantly increases after 6 hrs. of etoposide treatment and continues to rise with subsequent 24 hrs. of etoposide treatment. In addition, the fluorescence lifetimes of BODIPY-LD, with etoposide treatment, begin to increase and distinct lipid droplet populations form after 24 hrs. of etoposide treatment. Moreover, unlike in A549 cells, etoposide treatment of HEK 293T cells did not result in both highly viscous and highly non-viscous lipid droplet formation in single cells. Instead, each cell has its own population of lipid droplets with very similar intensity-weighted fluorescence lifetimes of BODIPY-LD.

## Synthesis of BODIPY-LD and spectral identification

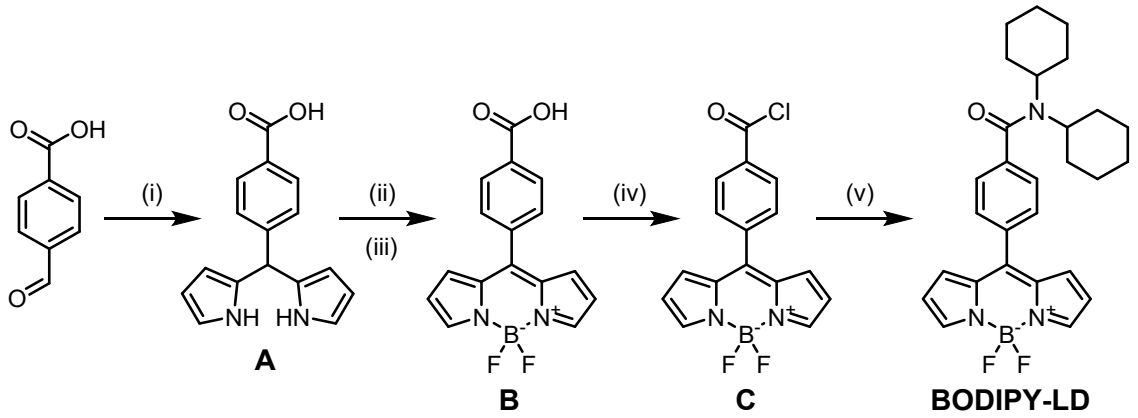


**Figure S10.** ***Reagents and conditions*****:** (i) 10 eq. of neat pyrrole, 0.1 M HCl, $CH_2Cl_2$, argon, r.t., 24 h; (ii) 1.5 eq. DDQ, $CH_2Cl_2$, and then (iii) 7 eq. $BF_3{\cdot}(OEt_2)_2$ and 7 eq. $Et_3N$, $CH_2Cl_2$, argon, 0 °C → r.t., darkness, 24 h; (iv) 2 eq. oxalyl chloride, 4 eq. $K_2CO_3$, drop of DMF, $CH_2Cl_2$, argon, r.t., 45 min; (v) 1.33 eq. dicyclohexylamine, 1.33 eq. DIPEA, $CH_2Cl_2$, argon, r.t., 24 h.

Compounds **A**, **B** [1] and **C** [2] were synthesized according to previously published procedures.

**BODIPY-LD.** Compound **C** (50 mg, 0.151 mmol) and 1.33 eq. of dicyclohexylamine (40.1 µl, 0.202 mmol) were dissolved in 2 mL of $CH_2Cl_2$ and 1.33 eq. of DIPEA (35.2 µL, 2.02 mmol) was added. The mixture was degassed with argon and stirred for 24 hours at room temperature. The reaction progress was controlled using thin-layer chromatography. After the reaction was complete, the solvent was removed under reduced pressure and the crude product was purified by column chromatography on silica gel (eluent – $CHCl_3$).

**BODIPY-LD.** Red-green crystals, yield 70 mg (97%), mp 260-261 °C, **$^1$H NMR** (400 MHZ, $CDCl_3$): δ (ppm) 7.97 (s, 2H); 7.61 (d, *J* = 8 Hz, 2H); 7.48 (d, *J* = 8 Hz, 2H); 6.95 (d, *J* = 4 Hz, 2H); 6.59 (d, *J* = 4 Hz, 2H); 3.50-3.00 (m, 2H); 2.65 (s, 2H); 1.99-1.48 (m, 12H), 1.43-0.92 (m, 6H). **$^{13}$C BMR** (100 MHz, $CDCl_3$): δ (ppm) = 170.0; 146.4; 144.4; 141.3; 134.8; 134.0; 131.5; 130.7; 125.8; 118.7; 31.3; 30.1; 26.6; 25.2. **$^{11}$B NMR** (128.4 MHZ, $CDCl_3$): δ (ppm) = 0.27 (t, $J_{B\text{-}F}$ = 28.9 Hz). **$^{19}$F NMR** (376.5 MHz, $CDCl_3$): δ (ppm) = -145.04 (dd, $J_{F\text{-}F}$ = 56.5 Hz, $J_{F\text{-}B}$ = 30.12 Hz).
**HRMS** (MALDI-TOF) m/z 476.23 ($C_{28}H_{33}BF_2N_3O^+$ $[M+H]^+$, requires 476.27).

## NMR spectra

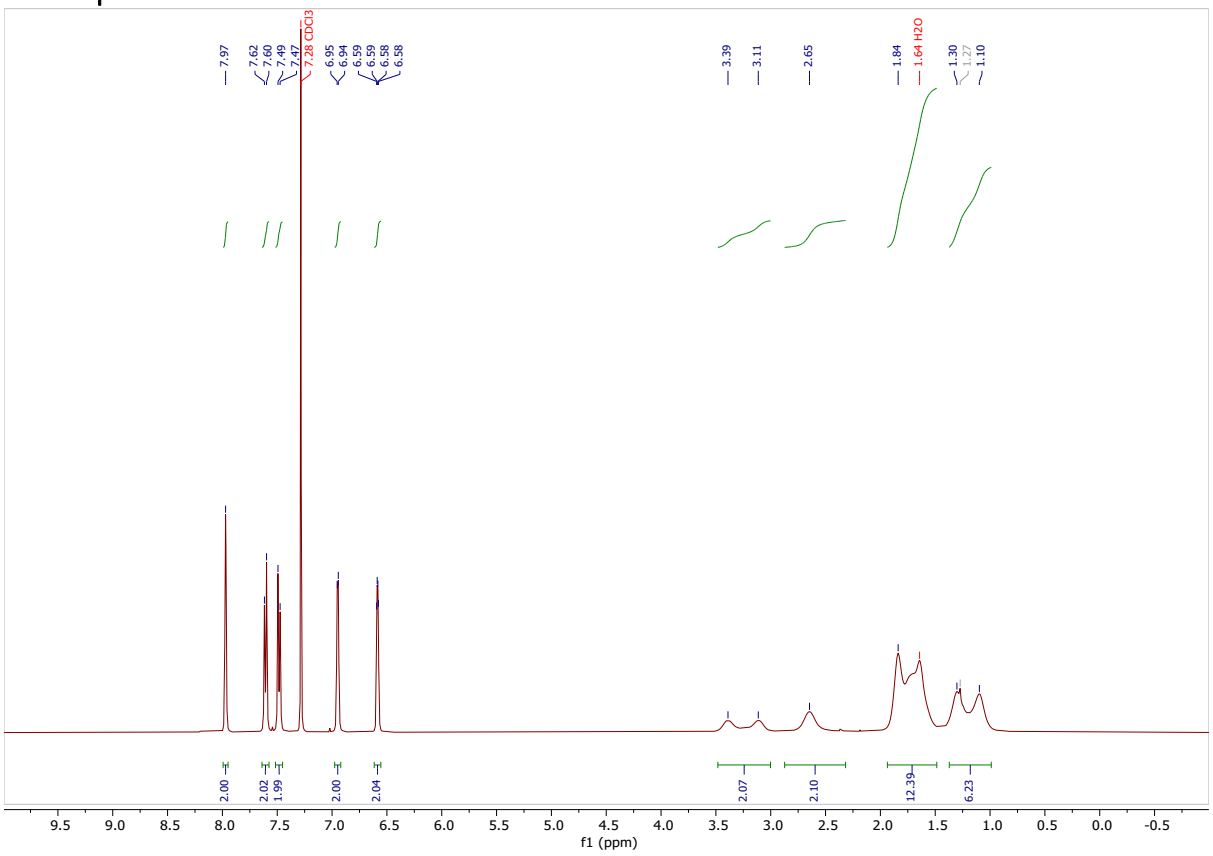


**Fig S11.** $^{1}$H NMR spectrum of **BODIPY-LD.**

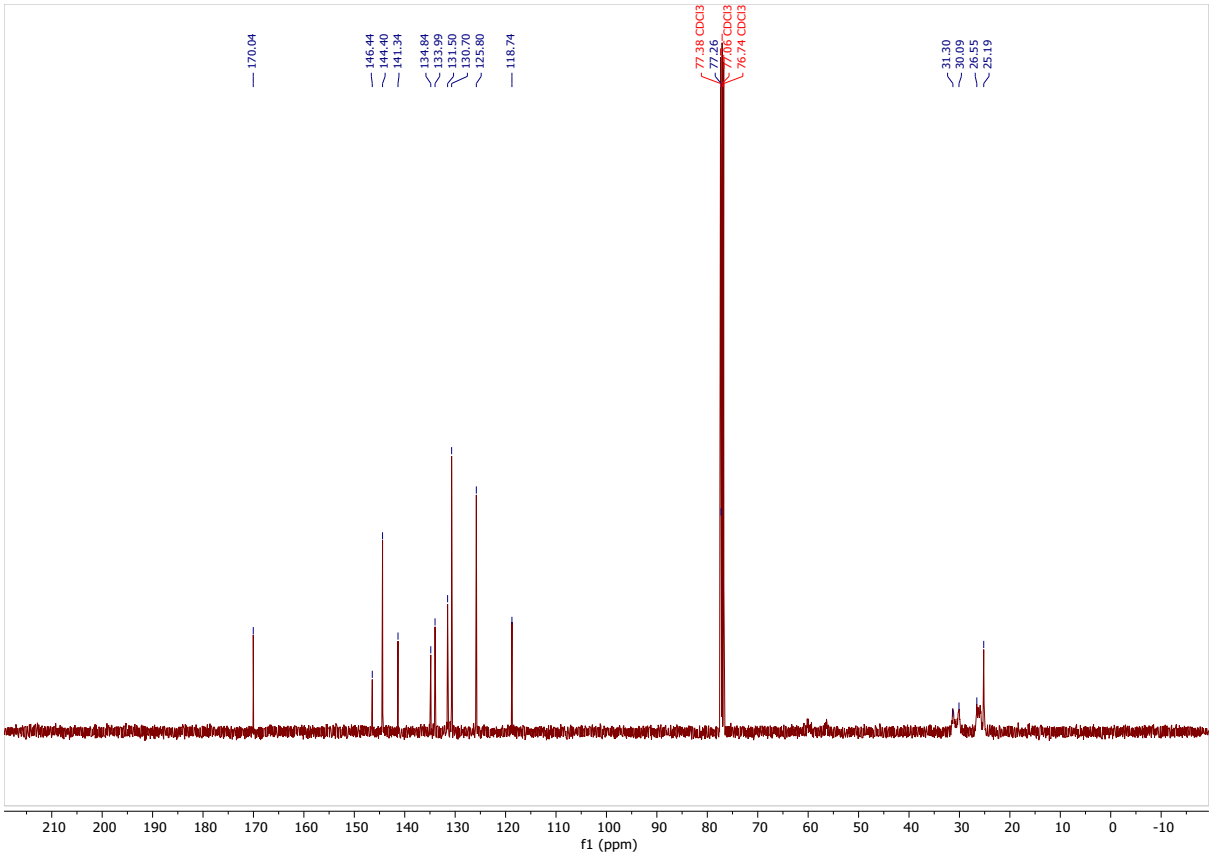


**Fig S12.** $^{13}C$ NMR spectrum of **BODIPY-LD.**

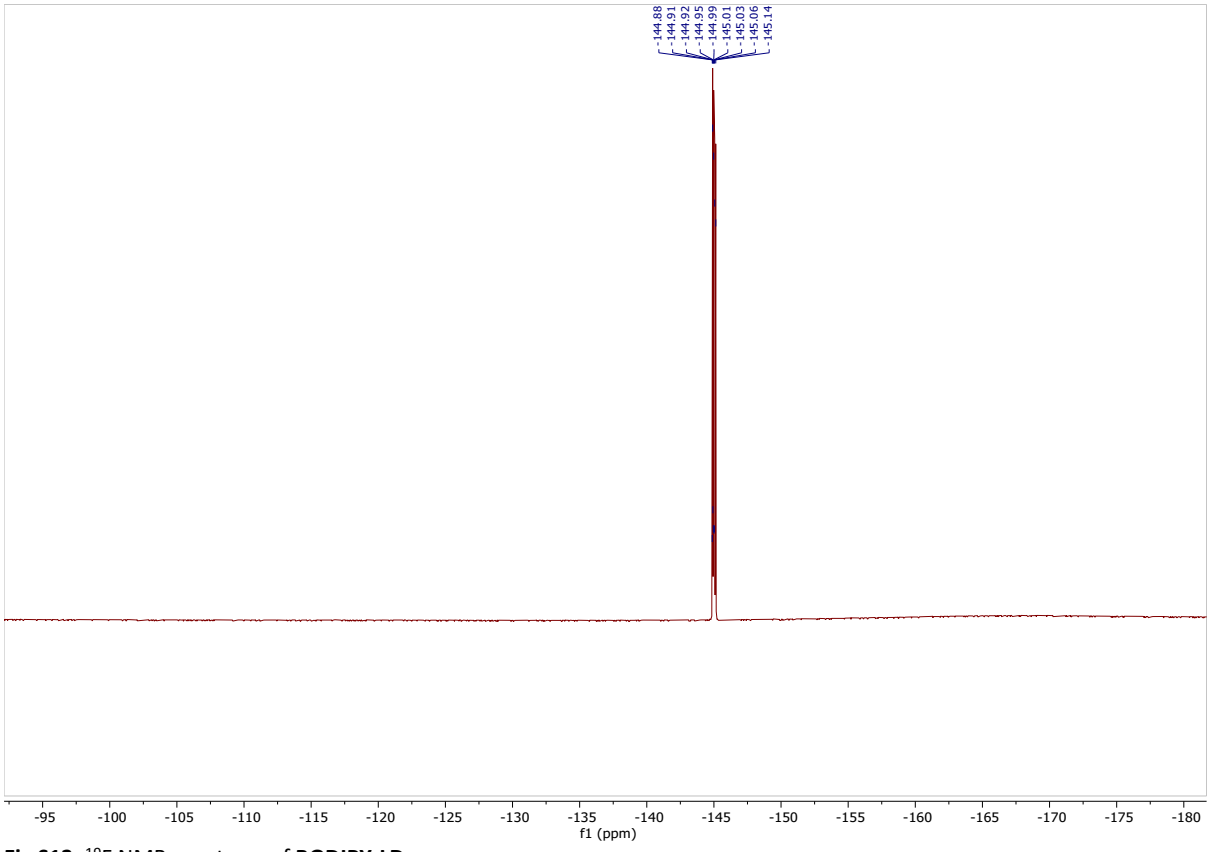


**Fig S13.** $^{19}F$ NMR spectrum of **BODIPY-LD.**

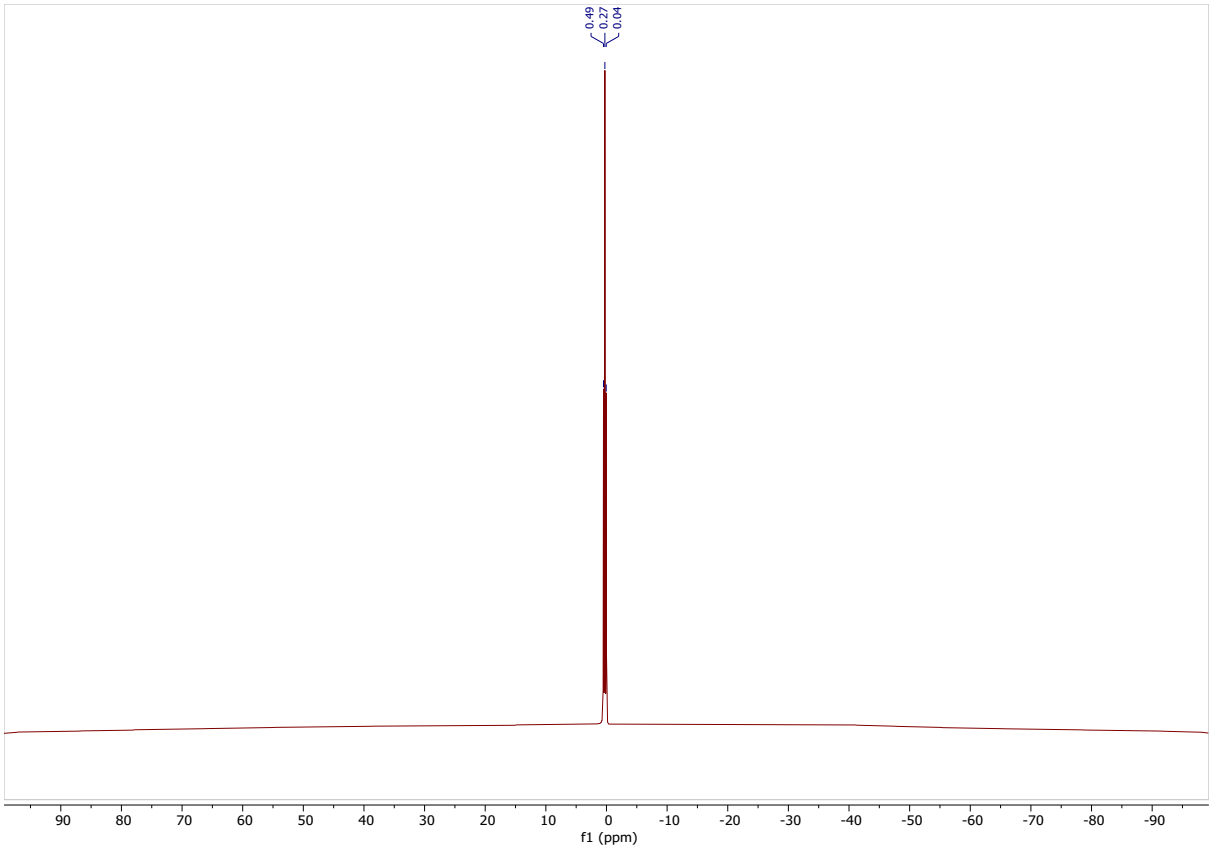


**Fig S14.** $^{11}$B NMR spectrum of **BODIPY-LD.**

## Mass Spectrometry (HPLC-MS) analysis

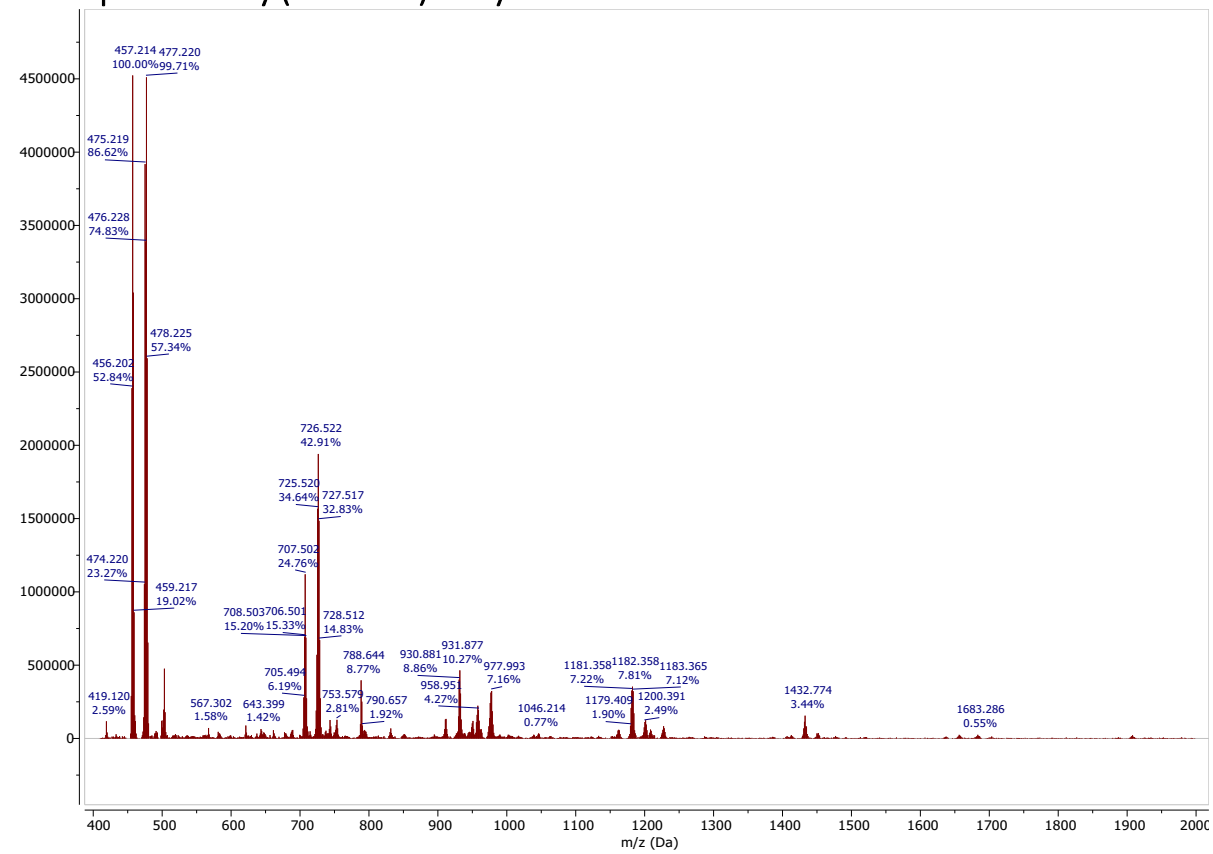

**Fig S15.** Mass spectrum of **BODIPY-LD**.

[1] M. Gruzdev, U. Chervonova, N. Bumagina, A. Kolker, Synthesis and Optical Properties of BODIPY with Active Group on meso- Position, Lett. Org. Chem. 13 (2016) 718–725. https://doi.org/10.2174/1570178614666161118155955.

[2] J. Pliquett, S. Amor, M. Ponce-Vargas, M. Laly, C. Racoeur, Y. Rousselin, F. Denat, A. Bettaïeb, P. Fleurat-Lessard, C. Paul, C. Goze, E. Bodio, Design of a multifunctionalizable BODIPY platform for the facile elaboration of a large series of gold(i)-based optical theranostics, Dalt. Trans. 47 (2018) 11203–11218. https://doi.org/10.1039/c8dt02364f.